IEEE Access
Multidisciplinary | Rapid Review | Open Access Journal

Received February 14, 2022, accepted March 3, 2022, date of publication March 8, 2022, date of current version March 25, 2022.

Digital Object Identifier 10.1109/ACCESS.2022.3157300

Collision Avoidance and Connectivity Preservation for Time-Varying Formation of Second-Order Multi-Agent Systems With a Dynamic Leader

RUIMIN ZHOU[1], WENQIAN JI[1], QINGZHENG XU[2], AND WENJIE SI[3]
[1]College of Information Engineering, Pingdingshan University, Pingdingshan 467000, China
[2]Faculty of Electrical Engineering and Computer Science, Ningbo University, Ningbo 315211, China
[3]School of Electrical and Control Engineering, Henan University of Urban Construction, Pingdingshan 467000, China

Corresponding author: Ruimin Zhou (zhoruimingreen@163.com)

This work was supported in part by the National Natural Science Foundation of China.

ABSTRACT In this paper, the problem of time-varying formation tracking control, with collision avoidance (CA) and connectivity preservation (CP), is studied for second-order multi-agent systems. Consider the unknown control input of virtual leader, an estimator is introduced to design a distributed time-varying formation tracking control protocol, while relaxing the condition the leader's velocity is constant. Different from some existing results, relative velocity-based action function is designed such that both CA and CP with small negative effects on formation are achieved, and a simpler method is proposed to eliminate the large jump and discontinuity of potential field force. Furthermore, the Lyapunov-like approach is used for the stability analysis and the theoretical results are derived. Accordingly, it is demonstrated that velocity tracking errors can asymptotically converge to 0, and steady-state position tracking errors are bounded and related to initial state. Finally, two simulation examples verify the effectiveness of theoretical results.

INDEX TERMS Multi-agent systems, collision avoidance, connectivity preservation, time-varying formation.

I. INTRODUCTION

With the superiority in terms of distribution, coordination and robustness, multi-agent systems (MASs) have numerous applications in the fields of intelligent logistics, military defense and disaster rescue, and have become the hottest research topic of distributed control systems in recent years. Generally, in the investigation of MASs, our attention is focused on the design of model-based or model-free control protocols such that cooperative tasks (e.g. consensus, formation, containment and flocking) are completed, while satisfying the system performance requirements [1]–[4]. Notice that, an interesting problem of MASs is how to realize CA and CP, because safety assurance is a prerequisite for other tasks.

When mobile agent performs task, it cannot obtain state information and surrounding environmental information in presence of unknown interference factors, which may cause path conflict and collision with other objects. Compared with obstacle avoidance, CA between agents is more difficult and challenging as a result of the unknown movement trends of moving agents. At present, for the collision problem of MASs, the popular solutions are behavior control method based on null space, model predictive control method and artificial potential field-based method. In behavior control approach, the missions to be accomplished have different priorities, and the low-priority task is projected onto the null space of CA task, so as to achieve the purpose of CA. At first, a series of results [5]–[7] were reported to detail the method design and theoretical proof. And then, behavior control approachs were applied to complete formation and collision tasks for MASs, UAVs and multiple spacecrafts [8]–[13]. Model predictive control approach considers distance constraints between agents for solving the optimal controller. Therefore, it can be realized that distances between agents are greater than predetermined safety distance [14]–[17]. In [18] and [19], the problem of formation control with CA for MASs was addressed by using distributed

The associate editor coordinating the review of this manuscript and approving it for publication was Zhan Bu.

model predictive control scheme, and the latter made a trade-off between the conflict objectives through introducing relaxation parameters into control Lyapunov function. Under model predictive control architecture, a bi-directional CA system was designed to minimize collision risk, and a dynamic weighted tuning strategy was also proposed in [20].

Compared with aforementioned two methods, the principle and implementation of artificial potential field-based method are simpler. In short, repulsive forces are applied to agents such that the agent separates from other agent's potential field [21]–[23], when their relative distances are less than the predefined value. In [24], a novel adaptive potential function was proposed to tune the critical variable. For networked Lagrangian systems, cooperative surrounding control problem with CA was handled in [25], by combining the adaptive technique and the potential functions. In the presence of unknown velocity and uncertainty, an observer-based sliding mode control law was proposed in [26], while ensuring that the relative distance of agents met the specified constraints. Different from the other works, the energy function including the relative position variable in [27] was presented to certify the effectiveness of the proposed CA method. In [28], based on distance and velocity, five cases of possible collision are firstly summarized, and a time-varying formation control law is proposed. However, the above results did not consider the controller jump problem, as a result of the discontinuities of potential field forces at potential field boundary. As is well known, the high-frequency change of control input will accelerate the wear of actuator, and has adverse effect on control performance. Therefore, it is of practical significance to propose an artificial potential field-based CA method, without large jump phenomenon.

In practical application scenarios, each agent is equipped with communication equipment, of which the communication ability is usually limited. For this reason, communication will be interrupted, if the distance between agents exceeds the threshold of communication range [29]–[31]. Though communication interruption can be restored automatically with appropriate relative distance, it has declined coordination performance of MASs. With second-order double-integral dynamics, a formation control law was proposed in [32], and the range of potential field function parameters was given, while achieving both CA and CP. Yu *et al.* [33] proposed a practical time-varying formation control protocol for high-order MASs, and the smooth of potential field forces was ensured. In [34], the trajectory tracking control law for unicycle robots was developed such that interagent collisions were avoided, and communications among agents were ensured. For autonomous surface vehicles [35], the problem of CA and CP was investigated based on output feedback. It is worth noting that the results of this paragraph only studied fixed formation with limitations in practical application. Furthermore, the dynamic of virtual leader was considered without control input, that is, its velocity was constant, which shows that the assumption condition is too strong.

In light of the above discussion and analysis, this paper proposes a time-varying formation protocol with CA and CP for second-order MASs, and a dynamic virtual leader is considered. The main innovations and contributions are summarized as follows:

1) Both CA and CP for time-varying formation are addressed, rather than only the CA problem was investigated in [24]–[27]. Furthermore, compared with [32] and [33], relative velocity is introduced to determine the risk of collision and communication interruption, as well as reduce the adverse effect of potential field forces on time-varying formation.
2) A novel and effective method is proposed to eliminate the large jump and discontinuity of potential field forces, and it is simpler compared with [33].
3) A dynamic leader is considered by using an estimator, which relaxes the condition in [28] that the leader's velocity is costant. Consequently, the application scenarios of time-varying foramtion are expanded and the corresponding theoretical results are derived.

The rest of this paper is arranged as follows. The preliminaries and problem formulation are given in Section II to more clearly illustrate the main results in Section III. Section IV is the important stability analysis results. Simulation results and conclusion are shown in Section V and Section VI, respectively.

Notation: In this paper, the symbols are all standard definitions. $\text{sign}(\cdot)$ is the sign function. $\|\cdot\|_p$ represents the p norm, and p is positive integer. I_n stands for the n-dimension identity matrix. ∇_x denotes the gradient along vector x. $\otimes$ is kronecker product. The index (t) for all the variables is omitted for simplicity in the appropriate case throughout the paper.

II. PRELIMINARIES AND PROBLEM FORMULATION

In this section, we first introduce graph theory, which will be used in subsection. And then, system model description and the objectives of this paper are provided.

A. GRAPH THEORY

In this paper, the communication between followers are two-way, so an undirected graph $G = (\mathcal{W}, \xi, \mathcal{A})$ is used to describe the interaction. $\mathcal{W}$ and ξ represent the edge set and vertex set, respectively. When there is an edge between agents i and j, one has $a_{ij} = a_{ji} = 1$, namely, they can exchange information with each other, otherwise $a_{ij} = a_{ji} = 0$. Notably, $a_{ii} = 0$. The adjacency matrix $\mathcal{A} \in \mathbb{R}^{N\times N}$ is composed of element a_{ij}. For the verification of resulting closed-loop system stability, the Laplace matrix $L = \mathcal{D} - \mathcal{A}$ is necessary to be introduced, where $\mathcal{D} = \text{diag}\{d_1, d_2, \cdots, d_N\}$ is the in-degree matrix with $d_i = \sum_{j=1}^{N} a_{ij}$, and the number of followers is N.

Assumption 1: At least one follower can obtain information from virtual leader, and the communication topology G is connected.

B. SYSTEM MODEL

Consider the MAS modeled by the following linear second-order double-integral system

$$\begin{cases} \dot{p}_0 = v_0 \\ \dot{v}_0 = u_0, i = 0 \end{cases} \tag{1}$$

$$\begin{cases} \dot{p}_i = v_i \\ \dot{v}_i = u_i, i = 1, \cdots, N, \end{cases} \tag{2}$$

where $p_i \in \mathbb{R}^m$, $v_i \in \mathbb{R}^m$ and $u_i \in \mathbb{R}^m$ are the position, velocity and control input of agent i, $i = 0, 1, \cdots, N$, respectively. The label 0 represents the virtual leader, and others are the followers.

Remark 1: It is noted that the velocity of virtual leader is time-varying, and so the motion forms of formation are varied. As a result, with the external reference signal (p_0 and v_0), the method design of formation tracking control is more complex, and application scenarios are wider compared with the existing works [24], [28], [29], [32], where the velocity of virtual leader is constant.

Assumption 2: [36] The control input of virtual leader is unknown to its followers, and it is bounded, namely, $\|u_0\|_2 \leq \xi$.

In order to describe the geometry of time-varying formation, $\tau_{\mathrm{p}i} \in \mathbb{R}^m$ is introduced, and it is the desired position offset between the follower i and virtual leader. Define the formation tracking error as

$$\begin{cases} e_{\mathrm{p}i} = p_i - p_0 - \tau_{\mathrm{p}i} \\ e_{\mathrm{v}i} = v_i - v_0 - \tau_{\mathrm{v}i}, \end{cases} \tag{3}$$

where $\tau_{\mathrm{v}i} \in \mathbb{R}^m$ is the desired velocity offset between the follower i and virtual leader. Obviously, $\tau_{\mathrm{v}i}$ can't always be 0 with the property of time-varying formation.

The goal of this paper is to provide a formation tracking control protocol for MAS (2) to achieve the desired formation, and two cases are presented. Furthermore, there are no collisions between followers, and the distance between followers does not exceed the maximum communication distance. One case is that, if $u_0 = 0$, $\lim_{t\to\infty} \|e_{\mathrm{p}i}(t)\|_2 = 0$ and $\lim_{t\to\infty} \|e_{\mathrm{v}i}(t)\|_2 = 0$ for all followers should be assured. Non-zero control input of virtual leader is considered in the other case, and it can be obtained $\lim_{t\to\infty} \|e_{\mathrm{p}i}(t)\|_2$ is bounded, as well as $\lim_{t\to\infty} \|e_{\mathrm{v}i}(t)\|_2 = 0$.

III. MAIN RESULTS

In this section, we first give the time-varying formation control protocol. Next, based on the principle of artificial potential field, the CA and CP scheme without large jump phenomenon of potential field forces, are presented, respectively.

A. TIME-VARYING FORMATION CONTROL PROTOCOL DESIGN

Consider that only a portion of followers connect directly with virtual leader, the following estimator is implemented to obtain the state estimation of virtual leader as

$$\begin{cases} \dot{\hat{p}}_{0,i} = \hat{v}_{0,i} - \epsilon_1 \mathrm{sign}\Big(\sum_{j=1}^{N} a_{ij}(\hat{p}_{0,i} - \hat{p}_{0,j}) \\ \qquad + b_i(\hat{p}_{0,i} - p_0)\Big) \\ \dot{\hat{v}}_{0,i} = -\epsilon_2 \mathrm{sign}\Big(\sum_{j=1}^{N} a_{ij}(\hat{v}_{0,i} - \hat{v}_{0,j}) \\ \qquad + b_i(\hat{v}_{0,i} - v_0)\Big), \end{cases} \tag{4}$$

where $\hat{p}_{0,i}$ and $\hat{v}_{0,i}$ are the ith follower's estimates of the position and velocity of virtual leader. ϵ_1 and ϵ_2 are parameters to be designed [36]. $b_i = 1$ denotes that follower i can obtain information from the virtual leader, otherwise $b_i = 0$. For analysis and description, the following auxiliary variables are introduced

$$\begin{cases} \zeta_{\mathrm{p}i} = \sum_{j=1}^{N} a_{ij}(e_{\mathrm{p}i} - e_{\mathrm{p}j}) + \hat{e}_{\mathrm{p}i} \\ \zeta_{\mathrm{v}i} = \sum_{j=1}^{N} a_{ij}(e_{\mathrm{v}i} - e_{\mathrm{v}j}) + \hat{e}_{\mathrm{v}i}, \end{cases} \tag{5}$$

where $\hat{e}_{\mathrm{p}i} = p_i - \hat{p}_{0,i} - \tau_{\mathrm{p}i}$, $\hat{e}_{\mathrm{v}i} = v_i - \hat{v}_{0,i} - \tau_{\mathrm{v}i}$. Then the time-varying formation control protocol is designed as follows

$$u_i^{\mathrm{f}} = k_1\zeta_{\mathrm{p}i} + k_2\zeta_{\mathrm{v}i} - k_3\mathrm{sign}(\hat{e}_{\mathrm{v}i}) + \dot{\tau}_{\mathrm{v}i}, \tag{6}$$

where k_1, k_2 and k_3 are the parameters to be designed.

Remark 2: The third term of (6) ensures that the velocity tracking error asymptotically converges to 0 in presence of the non-zero control input of virtual leader. So it can be removed with in the autonomous virtual leader case. As is known to all, $\lim_{t\to\infty} \hat{e}_{\mathrm{v}i}(t) \equiv 0$ is not established in practical application as a result of measure noise and estimated accuracy. Hence, the presence of $\mathrm{sign}(\hat{e}_{\mathrm{v}i})$ has an adverse effect on control input when $\hat{e}_{\mathrm{v}i}$ is small enough. To deal with this problem, we can remove the third term of (6) if the velocity tracking error $e_{\mathrm{v}i}$ satisfies our predefined precision.

B. COLLISION AVOIDANCE SCHEME DESIGN

As shown in Fig. 1, there is a virtual potential field around agent j with a radius r_{out}, and r_{out} is the safe distance between agents. When agent i is in the potential field of agent j, and the condition $\|v_i\|_2\cos\theta_{ij} + \|v_j\|_2\cos\theta_{ji} > 0$ holds, it will be subject to a repulsive force along $\overrightarrow{p_{ij}}$. Likewise, agent j will be subject to a repulsive force along $\overrightarrow{p_{ji}}$. θ_{ij} is the intersection angle between $\overrightarrow{v_i}$ and $\overrightarrow{p_{ji}}$. The chattering-free potential field function is designed as follows:

$$\Psi_{\mathrm{ca}} = \begin{cases} \int_{r_{\mathrm{out}}}^{\|p_{ij}\|_2} \phi_{\mathrm{ca}}(s)ds, \ \|p_{ij}\|_2 \in (2r, r_{\mathrm{out}}] \text{ and } \rho > 0 \\ \varpi_{\mathrm{ca}} \int_{\bar{r}}^{\|p_{ij}\|_2} \phi_{\mathrm{ca}}(s)ds, \ \|p_{ij}\|_2 \in (r_{\mathrm{out}}, \bar{r}] \text{ and } \rho > 0 \\ 0, \qquad \text{otherwise} \end{cases} \tag{7}$$

where $\rho = \|v_i\|_2 \cos\theta_{ij} + \|v_j\|_2 \cos\theta_{ji}$, and $\bar{r} > r_{\text{out}}$. Besides, ϖ_{ca} is the chattering-free factor to be given, and $\|p_{ij}\|_2$ represents the distance between agents i and j. The action function ϕ_{ca} is designed as

$$\phi_{\text{ca}} = \frac{-\delta_{\text{ca}}(1 - \exp(-\rho))}{(\|p_{ij}\|_2 - 2r + \mu)^2} \tag{8}$$

where δ_{ca} is a positive constant, and μ is a small enough positive constant to prevent that the denominator of (8) is 0. The chattering-free factor ϖ_{ca} is given by

$$\varpi_{\text{ca}} = 1 + \cos\Big(\frac{\|p_{ij}\|_2 - 2r_{\text{out}} + \bar{r}}{2(\bar{r} - r_{\text{out}})}\Big)\pi \tag{9}$$

Remark 3: Different from the previous works [24], [27], [28], [32], the potential field function (7) is divided into three sections to achieve chattering-free effect. We can have that from the action function (8), when the distance between agents is certain, the greater the relative velocity, the greater the potential field force. Therefore, the magnitude of the potential field force is determined jointly by the distance and the relative velocity. From Fig. 1 and Eqs. (7)-(9), it can be seen that it is a transient process, when $\|p_{ij}\|_2$ varies from r_{out} to $\bar{r}$. To be specific, ϖ_{ca} approaches 1 as $\|p_{ij}\|_2 \to r_{\text{out}}$, and it approaches 0 as $\|p_{ij}\|_2 \to \bar{r}$, which ensures that Ψ_{ca} is continuous at $\|p_{ij}\|_2 = \bar{r}$ and $\|p_{ij}\|_2 = r_{\text{out}}$, respectively. Therefore, the chattering phenomenon can be eliminated, and Eq. (9) is simpler than the results in [33].

Remark 4: ρ is the relative velocity between agents i and j, and it is introduced such that collision risk is accurately judged. The truth is, distance cannot be the only condition to determine the collision risk. Though the distance between two agents is very small, there is no collision risk in the case that two agents are stationary, as well as they move in the direction of increasing relative distance. Thus, the relative velocity and distance jointly determine the collision risk.

Consider other agents may collide with agent i at the same time, we get the CA control law of agent i as

$$u_i^{\text{ca}} = -\sum_{j \in N_i^{\text{ca}}} \nabla_{p_i} \Psi_{\text{ca}}(\|p_{ij}\|) \tag{10}$$

where N_i^{ca} is the CA neighbors, i.e., $N_i^{\text{ca}} = \{j | \|p_{ij}\|_2 \le \bar{r}\}$.

C. CONNECTIVITY MAINTENANCE SCHEME DESIGN

With the limited communication capacity, CP is necessary to complete the collaborative task. Consider that CP is the dual problem of CA, the scheme design procedure is similar to CA case. As shown in Fig. 2, with $\tilde{R} \le \|p_{ij}\|_2 \le R_{\text{out}}$ and $\rho < 0$, a potential field attractive force arises, which will make the distance between agents decrease. It is worth reminding that R_{out} is the radius of the maximum communication range, and $\tilde{R}$ is the communication interrupt warning radius. Based on the above description, the potential field function

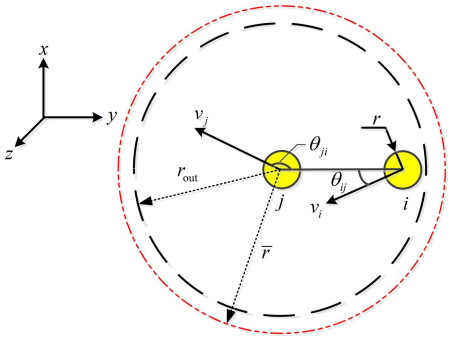

FIGURE 1. Chattering-free and velocity-based principle of CA.

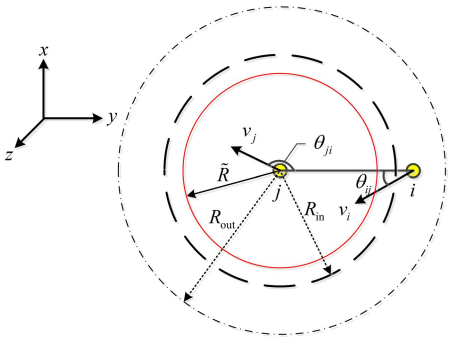

FIGURE 2. Chattering-free and velocity-based principle of CP.

for CP is

$$\Psi_{\text{conn}} = \begin{cases} \varpi_{\text{conn}} \displaystyle\int_{\tilde{R}}^{\|p_{ij}\|_2} \phi_{\text{ca}}(s)ds, \ \|p_{ij}\|_2 \in [\tilde{R}, R_{\text{in}}) \text{ and } \rho < 0 \\ \displaystyle\int_{R_{\text{in}}}^{\|p_{ij}\|_2} \phi_{\text{conn}}(s)ds, \ \|p_{ij}\|_2 \in [R_{\text{in}}, R_{\text{out}}) \text{ and } \rho < 0 \\ 0, \qquad \text{otherwise}, \end{cases} \tag{11}$$

where the adaptive action function ϕ_{conn} is designed as

$$\phi_{\text{conn}} = \frac{-\delta_{\text{conn}}(1 - \exp(\rho))}{(R_{\text{out}} - \|p_{ij}\|_2 + \mu)^2}, \tag{12}$$

where δ_{conn} is a positive constant. The chattering-free factor is given as follows

$$\varpi_{\text{conn}} = 1 + \cos\Big(\frac{\|p_{ij}\|_2 - 2R_{\text{in}} + \tilde{R}}{2(\tilde{R} - R_{\text{in}})}\Big)\pi. \tag{13}$$

The CP control input for the agent i is

$$u_i^{\text{conn}} = -\sum_{j \in N_i^{\text{conn}}} \nabla_{p_i} \Psi_{\text{conn}}(\|p_{ij}\|_2), \tag{14}$$

where $N_i^{\text{conn}} = \{j : \tilde{R} \le \|p_{ij}\|_2 < R_{\text{out}} \text{ and } j \in N_i\}$.

Combine the formation term (6), the CA term (10) and CP (14), we have

$$u_i = u_i^{\text{f}} + u_i^{\text{ca}} + u_i^{\text{conn}}. \tag{15}$$

IV. STABILITY ANALYSIS

Theorem 1: Under Assumptions 1 and 2, the controller (15) guarantees that the MAS (2) is globally asymptotically stable with zero steady-state velocity tracking errors, and position tracking errors satisfy $\lim_{t\to\infty}\sum_{i=1}^{N}\|e_{pi}\|_2 \le 2V_1(0)/\xi$, where $k_1 = -1$, $k_2 < 0$, $k_3 > \xi$, and $V_1(0)$ is the initial state of Lyapunov-like function V_1. Furthermore, CA and CP can be achieved.

Proof: Consider the following Lyapunov-like function V_1 as

$$V_1 = \frac{1}{2}\sum_{i=1}^{N}\Big(\sum_{j\in N_i^{\mathrm{ca}}}\Psi_{\mathrm{ca}}(\|p_{ij}\|_2) + \sum_{j\in N_i^{\mathrm{conn}}}\Psi_{\mathrm{conn}}(\|p_{ij}\|_2) + e_{\mathrm{p}i}^{\mathrm{T}}e_{\mathrm{p}i} + e_{\mathrm{v}i}^{\mathrm{T}}e_{\mathrm{v}i}\Big) + \frac{1}{2}E_{\mathrm{p}}^{\mathrm{T}}(L\otimes I_m)E_{\mathrm{p}}, \quad (16)$$

where $E_{\mathrm{p}} = [e_{\mathrm{p}1}^{\mathrm{T}}\ e_{\mathrm{p}2}^{\mathrm{T}}\ \cdots\ e_{\mathrm{p}N}^{\mathrm{T}}]^{\mathrm{T}}$, and then the time derivative of V_1 is

$$\begin{aligned}
\dot V_1 &= \frac{1}{2}\sum_{i=1}^{N}\Big(\sum_{j\in N_i^{\mathrm{ca}}}\frac{d\big(\Psi_{\mathrm{ca}}(\|p_{ij}\|_2)\big)}{d(\|p_{ij}\|_2)}\Big(\dot p_i^{\mathrm{T}}\frac{\partial\|p_{ij}\|_2}{\partial p_i} + \dot p_j^{\mathrm{T}}\frac{\partial\|p_{ij}\|_2}{\partial p_j}\Big)\\
&\quad + \sum_{j\in N_i^{\mathrm{conn}}}\frac{d\big(\Psi_{\mathrm{conn}}(\|p_{ij}\|_2)\big)}{d(\|p_{ij}\|_2)}\Big(\dot p_i^{\mathrm{T}}\frac{\partial\|p_{ij}\|_2}{\partial p_i} + \dot p_j^{\mathrm{T}}\frac{\|p_{ij}\|_2}{\partial p_j}\Big)\Big)\\
&\quad + \sum_{i=1}^{N}(e_{\mathrm{p}i}^{\mathrm{T}}\dot e_{\mathrm{p}i} + e_{\mathrm{v}i}^{\mathrm{T}}\dot e_{\mathrm{v}i}) + E_{\mathrm{p}}^{\mathrm{T}}(L\otimes I_m)\dot E_{\mathrm{p}}\\
&= \sum_{i=1}^{N}\Big\{\dot p_i^{\mathrm{T}}\Big(\sum_{j\in N_i^{\mathrm{ca}}}\nabla_{p_i}\Psi_{\mathrm{ca}}(\|p_{ij}\|_2) + \sum_{j\in N_i^{\mathrm{conn}}}\nabla_{p_i}\Psi_{\mathrm{conn}}(\|p_{ij}\|_2)\Big)\\
&\quad + e_{\mathrm{p}i}^{\mathrm{T}}e_{\mathrm{v}i} - e_{\mathrm{v}i}^{\mathrm{T}}u_0 - e_{\mathrm{v}i}^{\mathrm{T}}\dot\tau_{\mathrm{v}i} + e_{\mathrm{v}i}^{\mathrm{T}}\Big(k_1\sum_{j\in N_i}a_{ij}(e_{\mathrm{p}i} - e_{\mathrm{p}j})\\
&\quad + k_2\sum_{j\in N_i}a_{ij}(e_{\mathrm{v}i} - e_{\mathrm{v}j}) + k_1\hat e_{\mathrm{p}i} + k_2\hat e_{\mathrm{v}i} - k_3\mathrm{sign}(\hat e_{\mathrm{v}i})\\
&\quad + \dot\tau_{\mathrm{v}i} - \sum_{j\in N_i^{\mathrm{ca}}}\nabla_{p_i}\Psi_{\mathrm{ca}}(\|p_{ij}\|_2) - \sum_{j\in N_i^{\mathrm{conn}}}\nabla_{p_i}\Psi_{\mathrm{conn}}(\|p_{ij}\|_2)\Big)\Big\}\\
&\quad + E_{\mathrm{p}}^{\mathrm{T}}(L\otimes I_m)E_{\mathrm{v}}\\
&= \sum_{i=1}^{N}(v_i^{\mathrm{T}} - e_{\mathrm{v}i}^{\mathrm{T}})\Big(\sum_{j\in N_i^{\mathrm{ca}}}\nabla_{p_i}\Psi_{\mathrm{ca}}(\|p_{ij}\|_2)\\
&\quad + \sum_{j\in N_i^{\mathrm{conn}}}\nabla_{p_i}\Psi_{\mathrm{conn}}(\|p_{ij}\|_2)\Big) + \sum_{i=1}^{N}e_{\mathrm{p}i}^{\mathrm{T}}e_{\mathrm{v}i} - \sum_{i=1}^{N}e_{\mathrm{v}i}^{\mathrm{T}}u_0\\
&\quad + k_1\sum_{i=1}^{N}e_{\mathrm{v}i}^{\mathrm{T}}\sum_{j\in N_i}a_{ij}(e_{\mathrm{p}i} - e_{\mathrm{p}j}) + k_1\sum_{i=1}^{N}e_{\mathrm{v}i}^{\mathrm{T}}\hat e_{\mathrm{p}i}\\
&\quad + k_2\sum_{i=1}^{N}e_{\mathrm{v}i}^{\mathrm{T}}\sum_{j\in N_i}a_{ij}(e_{\mathrm{v}i} - e_{\mathrm{v}j}) + k_2\sum_{i=1}^{N}e_{\mathrm{v}i}^{\mathrm{T}}\hat e_{\mathrm{v}i}\\
&\quad - k_3\sum_{i=1}^{N}e_{\mathrm{v}i}^{\mathrm{T}}\mathrm{sign}(\hat e_{\mathrm{v}i}) + E_{\mathrm{p}}^{\mathrm{T}}(L\otimes I_m)E_{\mathrm{v}}. \quad (17)
\end{aligned}$$

With the undirected topology, the potential field force has no effect on the overall system (see [27], [28], [32]). Therefore, we have

$$V_2 = \sum_{i=1}^{N}(v_i^{\mathrm{T}} - e_{\mathrm{v}i}^{\mathrm{T}})\Big(\sum_{j\in N_i^{\mathrm{ca}}}\nabla_{p_i}\Psi_{\mathrm{ca}}(\|p_{ij}\|_2) + \sum_{j\in N_i^{\mathrm{conn}}}\nabla_{p_i}\Psi_{\mathrm{conn}}(\|p_{ij}\|_2)\Big) = 0. \quad (18)$$

Note that $\hat p_{0,i} = p_0$, $\hat v_{0,i} = v_0$ with the introduced estimator (4) when $t \ge T_1$ [36], and thus Eq. (17) can be rewritten as

$$\begin{aligned}
\dot V_1 &= k_1\sum_{i=1}^{N}e_{\mathrm{v}i}^{\mathrm{T}}\sum_{j\in N_i}a_{ij}(e_{\mathrm{p}i} - e_{\mathrm{p}j}) + (1+k_1)\sum_{i=1}^{N}e_{\mathrm{v}i}^{\mathrm{T}}e_{\mathrm{p}i}\\
&\quad + k_2\sum_{i=1}^{N}e_{\mathrm{v}i}^{\mathrm{T}}\sum_{j\in N_i}a_{ij}(e_{\mathrm{v}i} - e_{\mathrm{v}j}) + k_2\sum_{i=1}^{N}e_{\mathrm{v}i}^{\mathrm{T}}e_{\mathrm{v}i}\\
&\quad - \sum_{i=1}^{N}e_{\mathrm{v}i}^{\mathrm{T}}u_0 - k_3\sum_{i=1}^{N}e_{\mathrm{v}i}^{\mathrm{T}}\mathrm{sign}(e_{\mathrm{v}i}) + E_{\mathrm{p}}^{\mathrm{T}}(L\otimes I_m)E_{\mathrm{v}}\\
&= (1+k_1)E_{\mathrm{p}}^{\mathrm{T}}(L\otimes I_m)E_{\mathrm{v}} + k_2E_{\mathrm{v}}^{\mathrm{T}}(L\otimes I_m)E_{\mathrm{v}}\\
&\quad + (1+k_1)\sum_{i=1}^{N}e_{\mathrm{v}i}^{\mathrm{T}}e_{\mathrm{p}i} + k_2\sum_{i=1}^{N}\|e_{\mathrm{v}i}\|_2^2\\
&\quad - \sum_{i=1}^{N}e_{\mathrm{v}i}^{\mathrm{T}}u_0 - k_3\sum_{i=1}^{N}e_{\mathrm{v}i}^{\mathrm{T}}\mathrm{sign}(e_{\mathrm{v}i})\\
&= k_2E_{\mathrm{v}}^{\mathrm{T}}(L\otimes I_m)E_{\mathrm{v}} + k_2\sum_{i=1}^{N}\|e_{\mathrm{v}i}\|_2^2 - \sum_{i=1}^{N}e_{\mathrm{v}i}^{\mathrm{T}}u_0\\
&\quad - k_3\sum_{i=1}^{N}e_{\mathrm{v}i}^{\mathrm{T}}\mathrm{sign}(e_{\mathrm{v}i})\\
&\le k_2E_{\mathrm{v}}^{\mathrm{T}}(L\otimes I_m)E_{\mathrm{v}} + k_2\sum_{i=1}^{N}\|e_{\mathrm{v}i}\|_2^2 + \sum_{i=1}^{N}\|e_{\mathrm{v}i}\|_2\|u_0\|_2\\
&\quad - k_3\sum_{i=1}^{N}\|e_{\mathrm{v}i}\|_2\\
&\le k_2E_{\mathrm{v}}^{\mathrm{T}}(L\otimes I_m)E_{\mathrm{v}} + k_2\sum_{i=1}^{N}\|e_{\mathrm{v}i}\|_2^2\\
&\quad - (k_3 - \|u_0\|_2)\sum_{i=1}^{N}\|e_{\mathrm{v}i}\|_2\\
&\le 0 \quad (19)
\end{aligned}$$

where $\|e_{\mathrm{v}i}\|_1 > \|e_{\mathrm{v}i}\|_2$ and the property of L are used.

From (19), one has that V_1 is bounded and satisfies $V_1 \le V_1(0)$. Also, $\dot V_1 \to 0$ as $t \to \infty$ is implied. Then, $e_{\mathrm{v}i} \to 0$ as $t \to \infty$ are obtained with Eqs. (16) and (19).

If $\|p_{ij}\|_2 \to 2r$ or $\|p_{ij}\|_2 \to R_{\mathrm{out}}$, Ψ_{ca} or Ψ_{conn} will be infinite. Nevertheless, it has been proved V_1 is bounded. Consequently, CA and CP are ensured.

With $\lim_{t\to\infty} e_{vi} = 0$ and (15), we have

$$\begin{aligned}
&\lim_{t\to\infty}\sum_{i=1}^{N} e_{pi}^{T}(t)\dot{e}_{vi}(t)\\
&= \lim_{t\to\infty}\sum_{i=1}^{N} e_{pi}^{T}(t)(u_i(t)-u_0(t)-\dot{\tau}_{vi}(t))\\
&= -\lim_{t\to\infty} E_p^{T}(t)(L\otimes I_m)E_p(t) - \lim_{t\to\infty}\sum_{j\in N_i^{ca}} \nabla_{p_i}\Psi_{ca}(\|p_{ij}(t)\|_2)\\
&\quad -\lim_{t\to\infty}\sum_{j\in N_i^{conn}} \nabla_{p_i}\Psi_{conn}(\|p_{ij}(t)\|_2) - \lim_{t\to\infty}\sum_{i=1}^{N} e_{pi}^{T}(t)e_{pi}(t)\\
&\quad -\lim_{t\to\infty}\sum_{i=1}^{N} e_{pi}^{T}(t)u_0(t)\\
&= 0
\end{aligned} \tag{20}$$

Then from (16) and (20), one has

$$\begin{aligned}
\lim_{t\to\infty} V_1(t) &= \frac{1}{2}\lim_{t\to\infty}\Big(\sum_{i=1}^{N} e_{pi}^{T}(t)e_{pi}(t) + E_p^{T}(t)(L\otimes I_m)E_p(t)\Big)\\
&= -\frac{1}{2}\lim_{t\to\infty}\sum_{i=1}^{N} e_{pi}^{T}(t)u_0(t) \le V_1(0)
\end{aligned} \tag{21}$$

By using the properties of inequalities, $\lim_{t\to\infty}\sum_{i=1}^{N}\|e_{pi}(t)\|_2 \le 2V_1(0)/\xi$ is acquired. Thus, the proof is completed.

Remark 5: It is noted that the states of system (2) will not escape during $[0, T_1]$, and the detailed reason has been given in [37]. Hence, the proof process is omitted for simplicity.

Remark 6: To the best knowledge of authors, one of two following conditions should be satisfied such that the leader-follower formation tracking control can achieve zero steady-state tracking error. One is that all the followers can know the control input of the leader or estimate the states of the leader (see [39]–[41]), and the other is that the leader is autonomous (i.e. $u_0 = 0$) (see [42]–[44]).

Remark 7: For the method proposed in this paper, we can place agents in the positions in advance to make the initial energy (i.e. $V_1(0)$) as small as possible, so we can obtain the purpose of small formation steady-state position tracking error.

V. SIMULATION RESULTS

In this section, two simulation examples are employed to verify the effectiveness of the proposed scheme, of which the undirected communication topology is shown in Fig. 3. First, the fixed formation with an autonomous leader is considered in 2-D environment, and CA as well as CP is verified. Next, to be more general, the time-varying formation case is presented, with a dynamic leader in 3-D environment.

A. FIXED FORMATION WITH AN AUTONOMOUS LEADER IN 2-D ENVIRONMENT

In this example, the distances between agents are time-invariant if the formation is achieved. The desired formation is described by

$$\begin{cases}
\tau_{p1} = [0, 0]^T\\
\tau_{p2} = -7.5[\sqrt{3}, 1]^T\\
\tau_{p3} = -7.5[1, \sqrt{3}]^T\\
\tau_{p4} = -7.5[\sqrt{3}+\sqrt{2}, 1+\sqrt{2}]^T\\
\tau_{p5} = -7.5[1+\sqrt{2}, \sqrt{3}+\sqrt{2}]^T.
\end{cases}$$

The initial velocity of followers and the state of estimator (4), are all 0. The initial velocity of virtual leader is $[1.5\ 1.5]^T$, and the initial position is

$$\begin{cases}
p_0(0) = [2, -2]^T, & p_1(0) = [-4, -9]^T\\
p_2(0) = [0, 2]^T, & p_3(0) = [-2, 6]^T\\
p_4(0) = [-6, 1]^T, & p_5(0) = [-10, 1]^T.
\end{cases}$$

According to Theorem 1, relative parameters are selected as $k_1 = -1$, $k_2 = -0.3$, $r = 1$, $r_{out} = 5$, $\bar{r} = 6$, $R_{in} = 32$, $\tilde{R} = 35$, $R_{out} = 39$, $\delta_{ca} = 200$, $\delta_{conn} = 200$.

The simulation results are exhibited in Figs. 4-6. Fig. 4 shows the fixed formation trajectory of the MAS in 2-D environment. We can see that the five followers form a fixed formation like a boat, and the trajectory is a little abnormal in the initial stage due to the potential field forces. The evolution of distances between followers with/without CA and CP is revealed in Fig. 5, respectively. It can be seen from Fig. 5(a), agent 2 collides with agent 3 (e.g. $\|p_{23}\|_2 < 2r$) and the distances $\|p_{12}\|_2$ and $\|p_{13}\|_2$ are all greater than the radius of the maximum communication range (e.g. $\|p_{12}\|_2 > R_{out}$ and $\|p_{13}\|_2 > R_{out}$), when the algorithms of CA and CP are not introduced. For comparison, both CA and CP are achieved in Fig. 5(b), which reveals the validity of our proposed method. Furthermore, it is confirmed that in Fig. 6 zero steady-state formation tracking error can be achieved, when the control input u_0 of virtual leader is 0.

B. TIME-VARYING FORMATION WITH A DYNAMIC LEADER IN 3-D ENVIRONMENT

In this example, the initial position as well as the initial velocity of virtual leader, and the initial state of estimator, are all set to 0. The initial positions and velocities of followers are

$$\begin{cases}
p_1(0) = [7, 0.4, 1]^T, & v_1(0) = [0.1, 0, 0]^T\\
p_2(0) = [1, 4, -2]^T, & v_2(0) = [0, 0.4, 0]^T\\
p_3(0) = [3, -4, -5]^T, & v_3(0) = [0, 0.2, 0]^T\\
p_4(0) = [6, -2, -4]^T, & v_4(0) = [0.5, 0, 0]^T\\
p_5(0) = [0.6, 0, -8]^T, & v_5(0) = [0, 0.6, 0]^T,
\end{cases}$$

and the initial values of desired position offset are

$$\begin{cases}
\tau_{p1}(0) = [0, 0, 0]^T\\
\tau_{p2}(0) = [0, 8, -6]^T\\
\tau_{p3}(0) = [-4\sqrt{3}, -4, -6]^T\\
\tau_{p4}(0) = [4\sqrt{3}, -4, -6]^T\\
\tau_{p4}(0) = [0, 0, -12]^T.
\end{cases}$$

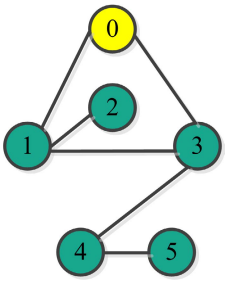

FIGURE 3. Communication topology.

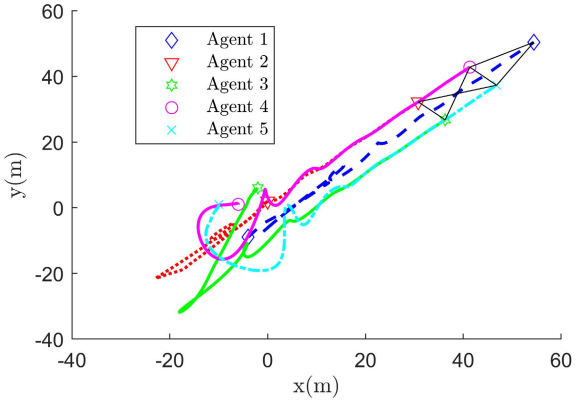

FIGURE 4. Fixed-formation trajectory of the MAS with an autonomous leader in 2-D environment.

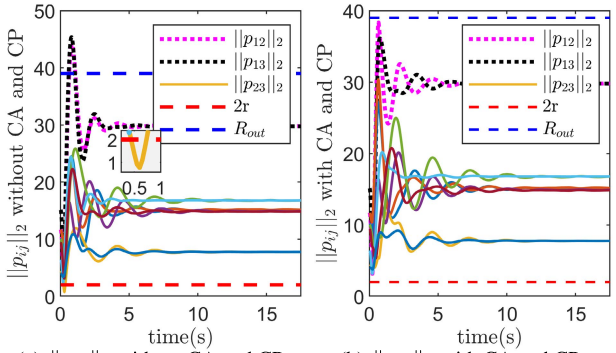

(a) $\|p_{ij}\|_2$ without CA and CP (b) $\|p_{ij}\|_2$ with CA and CP

FIGURE 5. The distances between followers with/without CA and CP.

The time-varying formation are described as

$$\begin{cases} \dot{\tau}_{\mathrm{v}1} = [0, 0, 0]^{\mathrm{T}} \\ \dot{\tau}_{\mathrm{v}2} = [0, \cos(0.5t), 0]^{\mathrm{T}} \\ \dot{\tau}_{\mathrm{v}3} = [-0.5\sqrt{3}\cos(0.5t), -0.5\cos(0.5t), 0]^{\mathrm{T}} \\ \dot{\tau}_{\mathrm{v}4} = [0.5\sqrt{3}\cos(0.5t), -0.5\cos(0.5t), 0]^{\mathrm{T}} \\ \dot{\tau}_{\mathrm{v}5} = [0, 0, 0]^{\mathrm{T}}. \end{cases}$$

The control input of virtual leader is $u_0 = [0, 0.2\sin(t) + 0.02, 0.5\sin(t) + 0.1]^{\mathrm{T}}$. To handle it, we set $k_3 = 5$, and other parameters are the same as the fixed formation case.

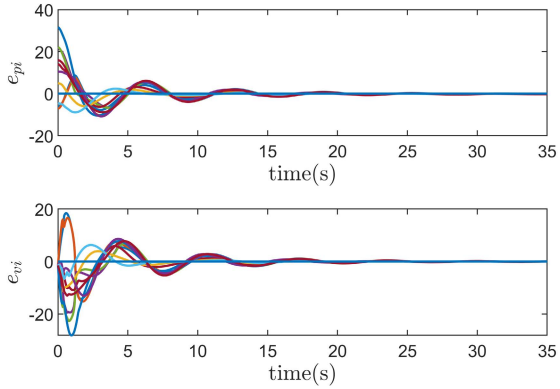

FIGURE 6. Position tracking errors and velocity tracking errors in 2-D environment.

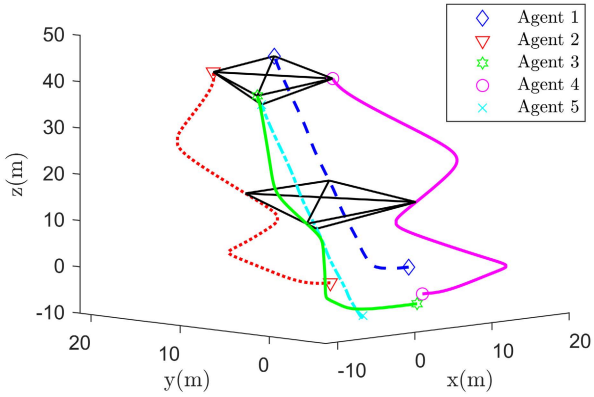

FIGURE 7. Time-varying formation trajectory of the MAS with a dynamic leader in 3-D environment.

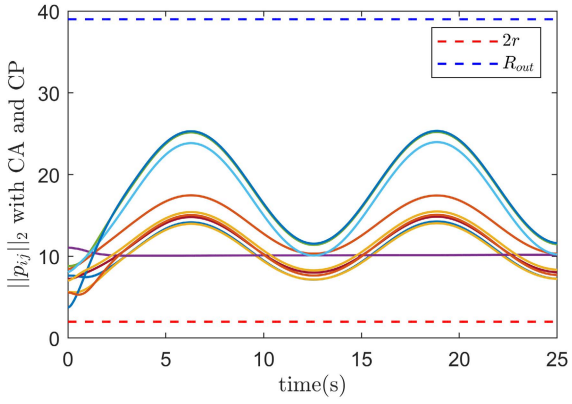

FIGURE 8. The distances between followers with CA and CP.

The simulation results are presented in Figs. 7-9. As shown in Fig. 7, the formation shape is time-varying in 3-D environment. In Fig. 8, the distances between followers accord with our prespecified formation (see $\tau_{\mathrm{p}1}(0)$ and $\dot{\tau}_{\mathrm{v}1}$). Note that, the algorithms of CA and CP do not work, because the distances between followers are always within a reasonable range in this simulation. Obviously, Fig. 9 is different

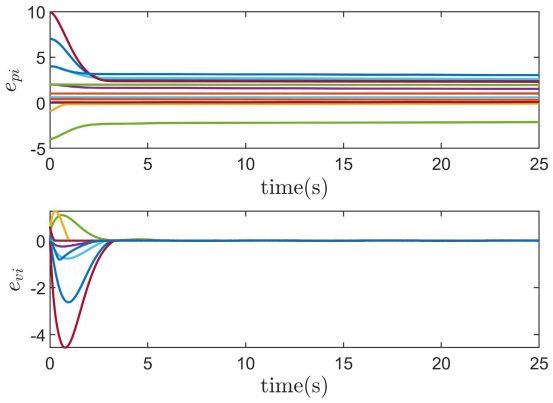

FIGURE 9. Position tracking errors and velocity tracking errors in 3-D environment.

from Fig. 6 in 2-D environment, because the virtual leader is dynamic. The velocity tracking errors converge to 0, and the steady-state position tracking errors satisfy the condition $\lim_{t\to\infty}\sum_{i=1}^{N}\|e_{pi}\|_2 \leq 2V_1(0)/\xi$ in *Theorem 1*. Therefore, we can reduce the steady-state position tracking errors by selecting appropriate initial state.

VI. CONCLUSION

This paper has investigated the time-varying formation problems of second-order MASs with a dynamic leader. Compared with existing works, the proposed formation control scheme can handle the unknown control input of virtual leader, in the case that not all followers can receive information from virtual leader. As a result, zero steady-state velocity tracking errors can be guaranteed, and the steady-state position tracking errors are within allowable domain with appropriate initial state. Also, CA as well as CP was ensured, and the large jump phenomenon of potential field force was eliminated. To validate the above results, two simulation examples including fixed formation and time-varying formation, were implemented. In the future, we will focus on the time-varying formation control problem with CA and CP for higher-order nonlinear MASs, while using the multi-objective optimization method [45]–[48].

REFERENCES

[1] A. Dorri, S. S. Kanhere, and R. Jurdak, "Multi-agent systems: A survey," *IEEE Access*, vol. 6, pp. 28573–28593, 2018.

[2] W. He, W. Xu, X. Ge, Q.-L. Han, W. Du, and F. Qian, "Secure control of multiagent systems against malicious attacks: A brief survey," *IEEE Trans. Ind. Informat.*, vol. 18, no. 6, pp. 3595–3608, Jun. 2022, doi: 10.1109/TII.2021.3126644.

[3] W. Zhang, Y. Zhao, W. He, and G. Wen, "Time-varying formation tracking for multiple dynamic targets: Finite- and fixed-time convergence," *IEEE Trans. Circuits Syst. II, Exp. Briefs*, vol. 68, no. 4, pp. 1323–1327, Apr. 2021.

[4] J. Cao, Z. Bu, Y. Y. Wang, H. Yang, J. C. Jiang, and H. J. Li, "Detecting prosumer-community groups in smart grids from the multiagent perspective," *IEEE Trans. Syst., Man, Cybern., Syst.*, vol. 49, no. 8, pp. 1652–1664, Aug. 2019.

[5] G. Antonelli, "Experiments of formation control with collisions avoidance using the null-space-based behavioral control," in *Proc. 14th Medit. Conf. Control Autom.*, Dec. 2006, pp. 1–6.

[6] F. Arrichiello, S. Chiaverini, and T. Fossen, "Formation control of underactuated surface vessels using the null-space-based behavioral control," in *Proc. IEEE/RSJ Int. Conf. Intell. Robots Syst.*, Oct. 2006, pp. 5942–5947.

[7] G. Antonelli, "Stability analysis for prioritized closed-loop inverse kinematic algorithms for redundant robotic systems," *IEEE Trans. Robot.*, vol. 25, no. 5, pp. 985–994, Oct. 2009.

[8] N. Zhou and Y. Xia, "Coordination control design for formation reconfiguration of multiple spacecraft," *IET Control Theory Appl.*, vol. 9, no. 15, pp. 2222–2231, Oct. 2015.

[9] J. Chen, M. Gan, J. Huang, L. Dou, and H. Fang, "Formation control of multiple Euler-Lagrange systems via null-space-based behavioral control," *Sci. China Inf. Sci.*, vol. 59, no. 1, pp. 1–11, 2016.

[10] M. C. P. Santos, C. D. Rosales, M. Sarcinelli-Filho, and R. Carelli, "A novel null-space-based UAV trajectory tracking controller with collision avoidance," *IEEE/ASME Trans. Mechatronics*, vol. 22, no. 6, pp. 2543–2553, Dec. 2017.

[11] J. Huang, N. Zhou, and M. Cao, "Adaptive fuzzy behavioral control of second-order autonomous agents with prioritized missions: Theory and experiments," *IEEE Trans. Ind. Electron.*, vol. 66, no. 12, pp. 9612–9622, Dec. 2019.

[12] W. Wang, C. Li, and Y. Guo, "Relative position coordinated control for spacecraft formation flying with obstacle/collision avoidance," *Nonlinear Dyn.*, vol. 104, no. 2, pp. 1329–1342, Apr. 2021.

[13] N. Zhou, X. Cheng, Z. Sun, and Y. Xia, "Fixed-time cooperative behavioral control for networked autonomous agents with second-order nonlinear dynamics," *IEEE Trans. Cybern.*, early access, Mar. 12, 2021, doi: 10.1109/TCYB.2021.3057219.

[14] P. Wang and B. Ding, "A synthesis approach of distributed model predictive control for homogeneous multi-agent system with collision avoidance," *Int. J. Control*, vol. 87, no. 1, pp. 52–63, Jan. 2014.

[15] H.-T. Zhang, Z. Cheng, G. Chen, and C. Li, "Model predictive flocking control for second-order multi-agent systems with input constraints," *IEEE Trans. Circuits Syst. I, Reg. Papers*, vol. 62, no. 6, pp. 1599–1606, Jun. 2015.

[16] H. Xiao, Z. Li, and C. L. P. Chen, "Formation control of leader–follower mobile robots' systems using model predictive control based on neural-dynamic optimization," *IEEE Trans. Ind. Electron.*, vol. 63, no. 9, pp. 5752–5762, Sep. 2016.

[17] J. Ji, A. Khajepour, W. W. Melek, and Y. Huang, "Path planning and tracking for vehicle collision avoidance based on model predictive control with multiconstraints," *IEEE Trans. Veh. Technol.*, vol. 66, no. 2, pp. 952–964, Feb. 2017.

[18] L. Dai, Q. Cao, Y. Xia, and Y. Gao, "Distributed MPC for formation of multi-agent systems with collision avoidance and obstacle avoidance," *J. Franklin Inst.*, vol. 354, no. 4, pp. 2068–2085, Mar. 2017.

[19] Y. Guo, J. Zhou, and Y. Liu, "Distributed Lyapunov-based model predictive control for collision avoidance of multi-agent formation," *IET Control Theory Appl.*, vol. 12, no. 18, pp. 2569–2577, Dec. 2018.

[20] G. Yu, P. K. Wong, J. Zhao, X. Mei, C. Lin, and Z. Xie, "Design of an acceleration redistribution cooperative strategy for collision avoidance system based on dynamic weighted multi-objective model predictive controller," *IEEE Trans. Intell. Transp. Syst.*, early access, Jan. 1, 2021, doi: 10.1109/TITS.2020.3045758.

[21] R. Olfati-Saber, "Flocking for multi-agent dynamic systems: Algorithms and theory," *IEEE Trans. Autom. Control*, vol. 51, no. 3, pp. 401–420, Mar. 2006.

[22] H. Su, X. Wang, and Z. Lin, "Flocking of multi-agents with a virtual leader," *IEEE Trans. Autom. Control*, vol. 54, no. 2, pp. 293–307, Feb. 2009.

[23] K. D. Do, "Coordination control of multiple ellipsoidal agents with collision avoidance and limited sensing ranges," *Syst. Control Lett.*, vol. 61, no. 1, pp. 247–257, Jan. 2012.

[24] A. Mondal, L. Behera, S. R. Sahoo, and A. Shukla, "A novel multi-agent formation control law with collision avoidance," *IEEE/CAA J. Autom. Sinica*, vol. 4, no. 3, pp. 558–568, Jul. 2017.

[25] C. Li, L. Chen, Y. Guo, and Y. Lyu, "Cooperative surrounding control with collision avoidance for networked Lagrangian systems," *J. Franklin Inst.*, vol. 355, no. 12, pp. 5182–5202, Aug. 2018.

[26] Y. Fei, P. Shi, and C.-C. Lim, "Robust and collision-free formation control of multiagent systems with limited information," *IEEE Trans. Neural Netw. Learn. Syst.*, early access, Sep. 29, 2021, doi: 10.1109/TNNLS.2021.3112679.

[27] Q. Shi, T. Li, J. Li, C. L. P. Chen, Y. Xiao, and Q. Shan, "Adaptive leader-following formation control with collision avoidance for a class of second-order nonlinear multi-agent systems," *Neurocomputing*, vol. 350, pp. 282–290, Jul. 2019.
[28] Z.-H. Pang, C.-B. Zheng, J. Sun, Q.-L. Han, and G.-P. Liu, "Distance- and velocity-based collision avoidance for time-varying formation control of second-order multi-agent systems," *IEEE Trans. Circuits Syst. II, Exp. Briefs*, vol. 68, no. 4, pp. 1253–1257, Apr. 2021.
[29] S. Su and Z. Lin, "Connectivity enhancing coordinated tracking control of multi-agent systems with a state-dependent jointly-connected dynamic interaction topology," *Automatica*, vol. 101, pp. 431–438, Mar. 2019.
[30] S. J. Yoo and B. S. Park, "Connectivity preservation and collision avoidance in networked nonholonomic multi-robot formation systems: Unified error transformation strategy," *Automatica*, vol. 103, pp. 274–281, May 2019.
[31] J. Fu, G. Wen, X. Yu, and Z.-G. Wu, "Distributed formation navigation of constrained second-order multiagent systems with collision avoidance and connectivity maintenance," *IEEE Trans. Cybern.*, early access, Jul. 6, 2020, doi: 10.1109/TCYB.2020.3000264.
[32] A. Mondal, C. Bhowmick, L. Behera, and M. Jamshidi, "Trajectory tracking by multiple agents in formation with collision avoidance and connectivity assurance," *IEEE Syst. J.*, vol. 12, no. 3, pp. 2449–2460, Sep. 2017.
[33] J. Yu, X. Dong, Q. Li, and Z. Ren, "Practical time-varying output formation tracking for high-order multi-agent systems with collision avoidance, obstacle dodging and connectivity maintenance," *J. Franklin Inst.*, vol. 356, no. 12, pp. 5898–5926, Aug. 2019.
[34] M. Karkoub, G. Atınç, D. Stipanovic, P. Voulgaris, and A. Hwang, "Trajectory tracking control of unicycle robots with collision avoidance and connectivity maintenance," *J. Intell. Robotic Syst.*, vol. 96, nos. 3–4, pp. 331–343, Dec. 2019.
[35] Z. Peng, D. Wang, T. Li, and M. Han, "Output-feedback cooperative formation maneuvering of autonomous surface vehicles with connectivity preservation and collision avoidance," *IEEE Trans. Cybern.*, vol. 50, no. 6, pp. 2527–2535, Jun. 2020.
[36] Y. Cao, W. Ren, and Z. Meng, "Decentralized finite-time sliding mode estimators and their applications in decentralized finite-time formation tracking," *Syst. Control Lett.*, vol. 59, no. 9, pp. 522–529, Sep. 2010.
[37] Y. Huang and Y. Jia, "Fixed-time consensus tracking control of second-order multi-agent systems with inherent nonlinear dynamics via output feedback," *Nonlinear Dyn.*, vol. 91, no. 2, pp. 1289–1306, 2018.
[38] G. Wen, C. L. P. Chen, and Y.-J. Liu, "Formation control with obstacle avoidance for a class of stochastic multiagent systems," *IEEE Trans. Ind. Electron.*, vol. 65, no. 7, pp. 5847–5855, Jul. 2018.
[39] J. Hu, P. Bhowmick, and A. Lanzon, "Distributed adaptive time-varying group formation tracking for multiagent systems with multiple leaders on directed graphs," *IEEE Trans. Control Netw. Syst.*, vol. 7, no. 1, pp. 140–150, Mar. 2020.
[40] Y. Hua, X. Dong, G. Hu, Q. Li, and Z. Ren, "Distributed time-varying output formation tracking for heterogeneous linear multiagent systems with a nonautonomous leader of unknown input," *IEEE Trans. Autom. Control*, vol. 64, no. 10, pp. 4292–4299, Oct. 2019.
[41] Z. Liu, Y. Li, F. Wang, and Z. Chen, "Reduced-order observer-based leader-following formation control for discrete-time linear multi-agent systems," *IEEE/CAA J. Automatica Sinica*, vol. 8, no. 10, pp. 1715–1723, Oct. 2021.
[42] Y. Hua, X. Dong, Q. Li, and Z. Ren, "Distributed adaptive formation tracking for heterogeneous multiagent systems with multiple nonidentical leaders and without well-informed follower," *Int. J. Robust Nonlinear Control*, vol. 30, no. 6, pp. 2131–2151, Apr. 2020.
[43] Y. Cai, H. Zhang, J. Zhang, and W. Wang, "Fixed-time leader-following/containment consensus for a class of nonlinear multi-agent systems," *Inf. Sci.*, vol. 555, pp. 58–84, May 2021.
[44] R. Yang, L. Liu, and G. Feng, "Leader-following output consensus of heterogeneous uncertain linear multiagent systems with dynamic event-triggered strategy," *IEEE Trans. Syst., Man, Cybern., Syst.*, vol. 52, no. 3, pp. 1626–1637, Mar. 2022, doi: 10.1109/TSMC.2020.3034352.
[45] Z. Bu, H.-J. Li, C. Zhang, J. Cao, A. Li, and Y. Shi, "Graph K-means based on leader identification, dynamic game, and opinion dynamics," *IEEE Trans. Knowl. Data Eng.*, vol. 32, no. 7, pp. 1348–1361, Jul. 2020.
[46] G. Wang, C. Wang, L. Li, and Z. Zhang, "Designing distributed consensus protocols for second-order nonlinear multi-agents with unknown control directions under directed graphs," *J. Franklin Inst.*, vol. 354, no. 1, pp. 571–592, Jan. 2017.
[47] G. Wang, C. Wang, and L. Li, "Fully distributed low-complexity control for nonlinear strict-feedback multiagent systems with unknown dead-zone inputs," *IEEE Trans. Syst., Man, Cybern., Syst.*, vol. 50, no. 2, pp. 421–431, Feb. 2020.
[48] G. Wang, "Distributed control of higher-order nonlinear multi-agent systems with unknown non-identical control directions under general directed graphs," *Automatica*, vol. 110, Dec. 2019, Art. no. 108559.

RUIMIN ZHOU received the B.E. degree in automation and the M.S. degree in control engineering from the Wuhan University of Technology, Wuhan, China, in 2012 and 2014, respectively. From 2015 to 2018, she was an Assistant Engineer with Pinggao Group Company Ltd. She is currently a Lecturer with the College of Information Engineering, Pingdingshan University. Her research interests include multi-agent systems and networked control systems.

WENQIAN JI received the Ph.D. degree in physical electronics from Nanjing Normal University, in 2021. In July 2021, she joined the School of Information Engineering, Pingdingshan University. Her research interest includes acoustic metamaterials.

QINGZHENG XU received the M.S. degree from the School of Electrical Engineering and Automation, Henan Polytechnic University, Jiaozuo, China, in 2015, and the Ph.D. degree from the College of Automation Engineering, Nanjing University of Aeronautics and Astronautics, Nanjing, China, in 2020. From 2020 to 2022, he was a Lecturer with the Faculty of Electrical Engineering and Computer Science, Ningbo University, Ningbo, China. His current research interests include flight control, preview control, information fusion, and networked control systems.

WENJIE SI received the B.S. and M.S. degrees in control theory and control engineering from Zhengzhou University, Zhengzhou, China, in 2008 and 2011, respectively, and the Ph.D. degree in control theory and control engineering from the South China University of Technology, Guangzhou, China, in 2015. He was an Assistant Professor with the School of Automation Science and Engineering, South China University of Technology. Since 2018, he has been an Associate Professor with the School of Electrical and Control Engineering, Henan University of Urban Construction. His current research interests include adaptive neural control, nonlinear control, and deterministic learning theory.